

Synthesis and characterization of ceramics from coal fly ash and incinerated paper mill sludge

Erika Furlani, Sergio Brückner, Dino Minichelli, Stefano Maschio *

Università di Udine, Dipartimento di Scienze e Tecnologie Chimiche, Via del Cotonificio 108, 33100 Udine, Italy

Received 6 June 2007; received in revised form 21 July 2007; accepted 21 August 2007

Available online 22 September 2007

Abstract

Powders obtained from coal fly ash and paper mill sludge were milled alone or in mixture, pressed into specimens and sintered. Fired materials were characterized by density, water absorption, shrinkage on firing, crystal structure, microstructure, strength, hardness and toughness. Samples made with paper mill sludge alone had a high sintering temperature, contained extended fractures after sintering and were not further studied. All the other compositions, sintered between 1130 and 1190 °C, showed low water absorption, density below 2.6 g/cm³, fair mechanical properties and contained several phases. More in particular, the material containing 25 wt% of coal ash and 75 wt% of powder from paper sludge displayed the best overall behaviour.

© 2007 Elsevier Ltd and Techna Group S.r.l. All rights reserved.

Keywords: A. Sintering; E. Structural applications; Coal fly ash; Paper mill sludge

1. Introduction

In 1987, as result of a popular referendum, Italian People excluded the use of nuclear source from the production of electric energy. In the following years the use of methane was, in general, preferred to that of oil or coal. Today, due to the high cost of oil and methane, coal has become convenient again, mostly in power stations, where abatement of the ash from the exhaust gases is possible. In fact, although carried out on high quality coal, combustion implies the production of a lot of fly ash. Italy recycles a great quantity of fly ash from coal combustion in the production of special cements for which Italy is one of the major producers in the world [1]. Nevertheless the great amount of CFA produced would also require alternative ways for recycling. One of them is vitrification in order to transform the original powder into a more environmentally benign product [2–4]. A second option is the production of traditional ceramics such as tiles using mixtures of CFA with other products [5–7]. In this case materials prepared must be

tested in order to investigate whether their physico-chemical properties satisfy the standard normally observed in the ceramic industry.

Paper mill sludge (PS), produced during paper production, is composed of mineral fillers, small cellulose fibres, water and organic compounds. Presently, PS is mainly dumped to landfill at high costs. Recycling PS would have beneficial effects for paper producers, reducing the cost of paper production and, regarding the environment, limiting the resort to landfill disposal. A possible reuse of PS is their blending with natural raw materials extracted from the ores in the production of bricks or cements [8–10], since the main constituent elements of PS are Al, Mg, Si and Ca, whose oxides are largely used in the ceramic industry.

The production of cements, concretes or bricks could be not a safe processing of waste to reach their environmental compatibility. In fact, it is known that bricks and concretes contain high porosity, through which water or moisture can penetrate and partially or totally dissolve some of the eventual toxic compounds present therein.

The production of monolithic ceramics, such as earthenware tiles with low residual porosity, i.e. low water absorption, could be a more suitable way for processing and/or, better, recycling.

With this goal in mind we have produced, by sintering, materials using powders from CFA and PS alone or in mixtures.

* Corresponding author.

E-mail addresses: erika.furlani@uniud.it (E. Furlani), bruckner@uniud.it (S. Brückner), dino.minichelli@uniud.it (D. Minichelli), Stef.maschio@uniud.it (S. Maschio).

Intermediate compositions were chosen in order to test if specific mixtures of the two different wastes resulted in products having much better properties than products made from the waste alone.

Fired materials were characterized in terms of shrinkage on firing, water absorption, apparent density, microstructure, crystal phases and some mechanical properties were measured as well.

2. Experimental procedure

PS was first incinerated by calcination at 850 °C for 2 h whereas CFA was used as received.

The two wastes were submitted to chemical elemental analyses, that were carried out with a Spectro Mass 2000 induced coupled plasma (ICP) mass spectrometer. Loss on ignition (LOI) was determined, for the PS calcined powders and the as received CFA, by a further thermal treatment at 1000 °C for 1 h.

In this work, powders of five different compositions were submitted to the ceramic processing: pure CFA, pure PS and three blends, namely 50 wt% CFA and 50% PS (hereafter called CFA50), 75 wt% CFA and 25% PS (called CFA75) and 25 wt% CFA and 75% PS (called CFA25). All compositions were homogenized by milling for 1, 3 and 5 h by a home-made attritor mill. Milling parameters were as follows: plastic container; highly pure alumina spheres; distilled water; 300 cycles/min. The milled suspensions were dried in an oven for 24 h at 80 °C. After milling, the particle size distribution of the powders was evaluated by an Horiba LA950 instrument. Dried powders were sieved through a 200 µm sieve and uniaxially pressed, by a laboratory press, at 100 MPa into cylindrical (height = 4 mm; diameter = 12 mm), or parallelepipedal (4 mm × 5 mm × 50 mm) samples; the former were used for sintering studies, the latter for investigation of the physico-mechanical behaviour.

Cylindric specimens were sintered for 1 h in air, by an electric muffle, investigating the thermal range of 1100–1400 °C in order to optimize the sintering temperature of each composition.

Axial (h) and radial (Φ) shrinkage on firing were evaluated, on cylindric specimens, by the ratios $h_0 - h_1/h_0$ and $\Phi_0 - \Phi_1/\Phi_0$ (subscripts 0 and 1 referring to the sample dimensions before and after sintering).

The apparent density of sintered specimens was determined by the Archimedes method whereas water absorption was determined by the EN99 test. In agreement with this procedure, sintered samples were first weighed in air (W_1), then put into a covered beaker and boiled in water, for 2 h. After boiling, samples were cooled into water to room temperature, dried with a cloth and weighted again (W_2). Water absorption was evaluated as: $W(\%) = 100 (W_2 - W_1/W_1)$.

Mechanical properties were measured on materials fired at their optimal sintering temperature. Rupture strength (σ) was evaluated, on parallelepipedal specimens, by 4-point bend test with a crosshead speed of 0.2 mm/min using a Shimadzu AG10 equipment; Vickers hardness (H_v) was determined by a 100 N

load with a Zwick indenter on polished surfaces (6 µm diamond paste); fracture toughness (K_{IC}) was determined by the Indentation Strength in Bending (ISB) method, breaking parallelepipedal specimens indented with a load of 100 N. All mechanical data reported in the present research are averages of 10 measurements each.

Microstructures of the sintered samples were examined by an Assing Stereoscan scanning electron microscope (SEM). Crystal phases of the fired materials were investigated by X-ray diffraction (XRD) analysis which was performed on a Panalytical X'pert Pro Detector X'celerator. Monochromated $\text{CuK}\alpha_1$ was obtained by setting 40 kV and 40 mA operating conditions. SEM analysis and X-ray diffraction were performed on the same surface for all the specimens; it means that we have leaned the specimens (cylinders) on an alumina support for sintering and made X-rays and SEM, after sintering, on the opposite face.

3. Results and discussion

Chemical compositions (data are reported in terms of oxides) and LOI of the two starting powders are given in Table 1. It can be observed that PS contains great quantities of CaO , SiO_2 and Al_2O_3 , whereas CFA is characterized by large amounts of SiO_2 , Al_2O_3 and Fe_2O_3 . It can be also observed that both powders contain small amounts of toxic compounds. The LOI of the two powders is low, thus confirming that calcination of PS causes the decomposition of low contents of organic matter and soluble salts (carbonates, sulphates, chlorides, etc.) present in the received material.

Original powders require comminution of particles and homogenization, before pressing. The effect of milling time on mixtures containing 50 wt% CFA and 50% PS is reported in Fig. 1 where it is possible to compare the particle size distributions of powders milled for 1, 3 and 5 h. It can be

Table 1
Composition (wt%) and LOI (%) of the two starting powders

Component	PS	CFA
SiO_2	29.1	60.03
CaO	43.13	2.2
Al_2O_3	16.45	20.12
MgO	2.67	2.31
Fe_2O_3	2.45	8.85
ZrO_2	1.97	<0.01
Cr_2O_3	1.06	<0.01
TiO_2	0.42	0.89
SrO	0.22	<0.01
MnO_2	0.07	<0.01
SnO	0.06	0.02
Na_2O	0.03	0.58
K_2O	0.05	2.05
P_2O_5	<0.01	0.21
SO_3	0.04	2.14
Cl^-	<0.01	0.03
Undetermined	0.08	0.07
LOI	1.78	0.59

Excluding chlorine, elements are reported as oxides; those not reported in the table were determined in quantity lower than 0.01 wt%.

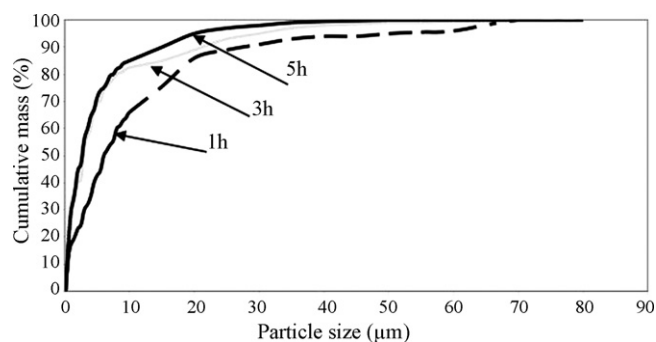


Fig. 1. Particle size distribution as function of the milling time of the powder with the composition 50 wt% CFA and 50% PS.

observed that, after a 3-h milling the amount of particles with a size larger than 50 μm is low. For longer milling, the gain of small at the expense of coarse particles is limited. This behaviour is similar for all compositions (the experimental results obtained on the other compositions are not reported in the present paper), therefore we set the milling time at 3 h, being aware that particle size distribution could be restricted increasing the milling time, but paying a cost in terms of milling energy.

Table 2 shows that the sintering temperatures range from 1130 to 1350 $^{\circ}\text{C}$. More in particular, it can be observed that samples prepared using PS alone have the highest sintering temperature (1350 $^{\circ}\text{C}$) and fired materials show the presence of extended fractures, as can be seen in Fig. 2. The former item is due to the chemical composition of PS alone, which contains large quantities of high melting compounds (i.e. CaO , Al_2O_3 , MgO , ZrO_2 , Cr_2O_3) and low amounts of low melting compounds (i.e. Na_2O , K_2O , etc.). The latter item depends on the presence of CaO and SiO_2 which react during the sintering to form 2CaO , SiO_2 . This is a polymorph component that transforms, on cooling, into a phase having a larger specific volume [11]. This transformation causes extended fractures in the fired material, therefore we do not further report on the characterization of PS alone. All other compositions were fired to a low residual porosity (low water absorption) in a narrower range of temperatures (1130–1190 $^{\circ}\text{C}$).

It must be pointed out that CFA alone has the lowest sintering temperature (1130 $^{\circ}\text{C}$), but in this case it is difficult to set the temperature for the sintering process. In fact, fired samples maintain a high residual porosity up to 1110 $^{\circ}\text{C}$



Fig. 2. Image of the fired samples. To the right there is the specimen obtained from PS alone showing extended fractures. To the left is set the sample made using CFA alone. In the middle are placed samples with intermediate compositions.

(water absorption $>20\%$). After sintering at 1130 $^{\circ}\text{C}$ (assumed as optimal sintering temperature) they contain a high amount of vitreous phase (see below). They are completely vitrified, losing their original shape, after sintering at 1140 $^{\circ}\text{C}$. Intermediate compositions show a progressive decrease of water absorption until the optimal sintering temperature (reported in Table 2) before losing the shape due to the formation of a high quantity of liquid phase during sintering.

Fig. 2 also shows that the colour of the fired samples ranges from brown (CFA alone) to creamy (PS alone) covering a series of different tonalities of yellow in the intermediate compositions. The brown colour of the CFA alone is due to the high content (8.8 wt%) of Fe_2O_3 in the original powder.

XRD analysis, done on the free surface of the sintered samples, reveals the presence of several phases in each material, as displayed in Fig. 3, nevertheless, for each composition, we mention only phases that were identified by a minimum of five representative peaks and in sufficiently good agreement with the corresponding PDF files.

More in particular, materials made of CFA alone contain a high amount of glass and a low content of polycrystalline phases; in this case, due to the high background noise, it was not possible to make a doubtless identification of any specific crystal structures.

Composition CFA 25 contains gehlenite (PDF 01-079-1726) as major phase. Gehlenite and anorthite (PDF 00-010-0378) are present in CFA 50 whereas anorthite and augite (PDF 01-078-1391) are the major phases of CFA 75. X-ray diffraction patterns revealed, in all compositions, also the presence of glass

Table 2

Sintering temperature, axial and radial shrinkage on firing, apparent density (ρ), water absorption, rupture strength (σ), Vickers hardness (H_v), and fracture toughness (K_{IC}) values measured in the sintered specimens

Sintered materials	Sintering temperature ($^{\circ}\text{C}$)	Axial shrinkage on firing (%)	Radial shrinkage on firing (%)	ρ (g/cm^3)	Water absorption (%)	σ (MPa)	H_v (GPa)	K_{IC} (MPa/m)
CFA	1130	12.8	12.7	1.94	1.8	58 ± 7	3.7 ± 0.1	0.9 ± 0.1
CFA75	1160	16.7	15.4	2.58	5.4	53 ± 4	4.6 ± 0.25	1.7 ± 0.25
CFA50	1168	14.2	13.1	2.16	6.2	49 ± 6	5.1 ± 0.3	2.9 ± 0.3
CFA25	1190	15.6	14.6	2.51	2.3	67 ± 3	6.3 ± 0.3	2.1 ± 0.1
PS	1350	nd	nd	nd	nd	nd	nd	nd

nd, data not determined.

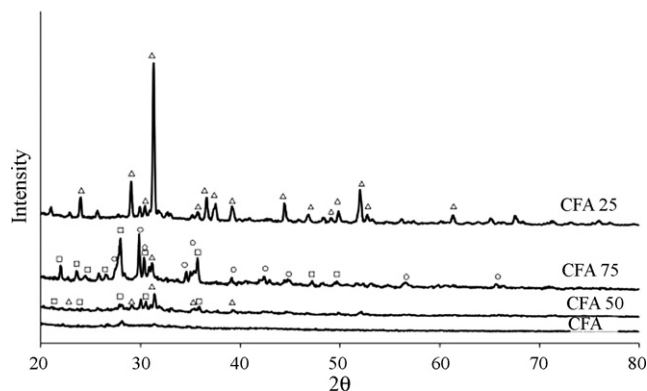


Fig. 3. X-ray diffraction patterns of the as fired surfaces of the samples. Symbols used to identify the phases are as follows: (Δ) = gehlenite, (\square) = anorthite, (\circ) = augite.

and other crystalline phases, but we have not been able to identify them unambiguously.

Axial and radial shrinkage on firing were measured after sintering at the optimal temperature of each composition. Radial shrinkage on firing ranges from 12.7% for CFA alone to 15.4% for CFA 75; axial shrinkage is close, but higher than radial shrinkage ranging from 12.8% for CFA alone to 16.7% for CFA 75: in both cases, values are higher than the ones generally required for the industrial production of all traditional ceramics [12]. It is noteworthy that CFA, containing a high amount of amorphous phase, has the lowest shrinkage values.

Density is 1.94 g/cm³ for CFA alone, 2.51 for CFA 25, 2.16 for CFA 50 and 2.58 for CFA 75. Density is a function of chemical composition, but also of total porosity which is the sum of open and close porosity. Open porosity can be evaluated by the measurement of water absorption which ranges from 1.8% for CFA alone to 6.2% for CFA 50. It can be observed that CFA has a low open porosity (water absorption = 1.8%), but a high total porosity because its density is low (1.94 g/cm³). It must also be pointed out that the water absorption test requires boiling in water. The process could induce dissolution of some soluble salts and determine a measured amount of water corresponding to a higher level of apparent porosity than is

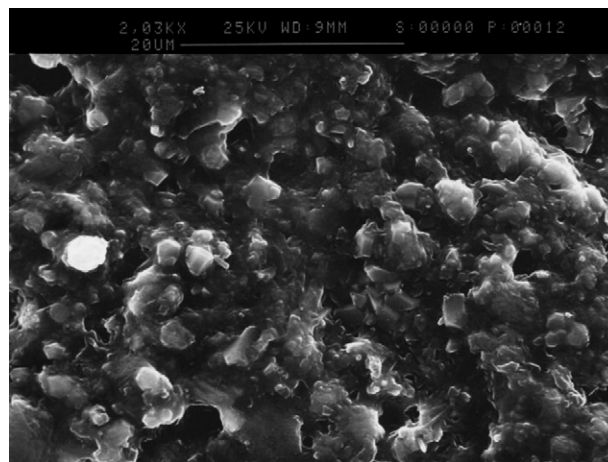


Fig. 5. SEM micrograph showing the surface of the sintered CFA25.

really present. Nevertheless, assuming as constant in all compositions the amount of soluble salts, the increase of water absorption could correspond to an increase of apparent porosity. More in particular, composition CFA 50 has an apparent density of 2.16 g/cm³ and water absorption of 6.2%. Both values indicate that the material is porous, but compatible with the industrial production of earthenware tiles [12]. If, in order to decrease porosity, we fired this material at temperatures higher than 1168 °C it would lose its original shape due to the formation of a high quantity of liquid phase during the sintering.

SEM photographs, made on free surfaces of the fired samples, are reported in Figs. 4–7. In CFA grains are not visible (see Fig. 4), but a continuous vitreous layer can be seen, covering the polycrystalline phases which are present, but are not identified by X-ray analysis. There is no evident porosity in agreement with the low water absorption. Samples made of CFA25, CFA50 and CFA75 (Figs. 5–7) contain both polycrystalline grains and glassy phases. SEM micrographs show that the vitreous phase is mainly concentrated along the surface of the fired specimens where they are not perfectly defined, being partially hidden by a thin layer of glass.

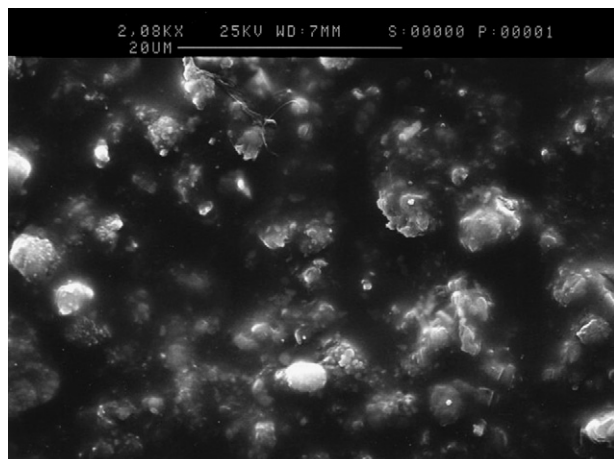


Fig. 4. SEM micrograph showing the surface of fired CFA alone.

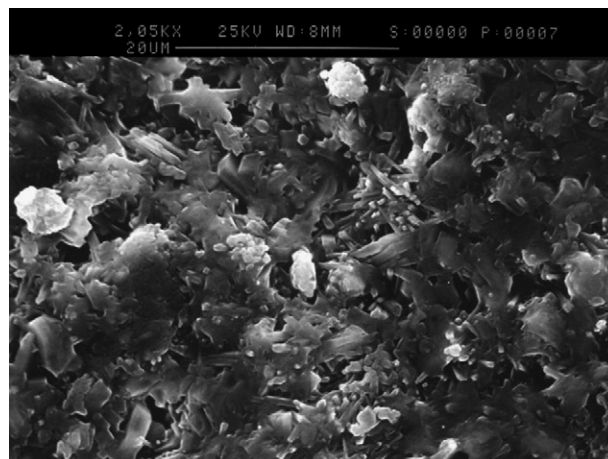


Fig. 6. SEM micrograph showing the surface of sintered CFA50.

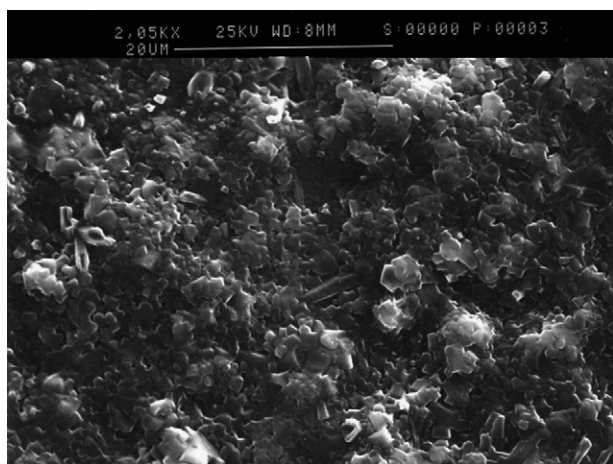


Fig. 7. SEM micrograph showing the surface of the sintered CFA75.

Some elongated grains are visible in compositions CFA50 and CFA75, not in CFA25; their amount is high in CFA50, low in CFA75. Equiaxial grains (polycrystals) of size smaller than $3\text{ }\mu\text{m}$ are visible in CFA25, CFA50 and CFA75. A certain superficial porosity can be observed in all these three compositions, but the sample made of CFA 25 looks less porous than those made of CFA50 and CFA75. Superficial porosity, in the sample made of CFA25, looks uniformly dispersed and of very small size ($\ll 1\text{ }\mu\text{m}$) whereas that of CFA50 and CFA 75 appears of larger size ranging from 1 to $3\text{ }\mu\text{m}$ in the former and from 1 to $5\text{ }\mu\text{m}$ in the latter. All these microstructures are in agreement with water absorption data and XRD analysis. The presence of many elongated grains, probably due to well developed gehlenite crystals [13] in CFA50, explains the low level of densification of this composition: elongated grains act as rigid inclusions and retard sintering. In our case, complete melting of the crystals occurs before the complete densification of this material.

CFA is mainly vitreous: it is reasonable that its mechanical properties depend on the properties of the vitreous phase and on the amount of total porosity. It is known that glass has low toughness and hardness, whereas strength is function of the size of the critic defect. Table 2 shows that hardness and toughness of CFA alone are low whereas strength is fair. This behaviour is due to the low apparent porosity (low water absorption), but significative total porosity (low density) that we measured in this composition.

Compositions CFA25, CFA50 and CFA75 are mainly polycrystalline and the vitreous phase is concentrated at the grain boundaries. The mechanical properties of these materials are influenced by: (i) properties of the vitreous phase; (ii) amount of total porosity and (iii) properties of the crystalline phases. Other researchers [13–15] demonstrated that materials where anorthite is the major phase behave better than those containing a great amount of gehlenite. As a consequence of that literature, mechanical properties of CFA 50 and CFA 75 are expected to be better than those of CFA 25. Unexpectedly, CFA 25 has the highest strength and hardness values. It means that the mechanical behaviour of our materials is influenced by the amount of total porosity and by the properties of the vitreous

phase more than by the quality of the phases therein contained. We can nevertheless observe that, CFA50 is the composition with the highest water absorption and we therefore may assume that it has the highest total porosity, which limits the possible rupture strength. On the contrary, the presence of pores, in addition to the presence of many elongated crystals, have beneficial effects on the toughness of this composition which shows the highest fracture toughness. In agreement with literature, it is known that a high residual porosity can increase fracture toughness of brittle materials with respect to same materials sintered to fully dense bodies. The introduction of elongated structures in brittle matrices is a common practice in the field of brittle matrix composites when fracture toughness of matrices must be improved. CFA50 contains equiaxial grains and vitreous phase (matrix) in which elongated structures (reinforcements) are dispersed and act in synergy with the not negligible residual porosity thus raising toughness.

In definitive, the mechanical characterization of the materials examined in the present research show that composition CFA25, CFA50 and CFA75 have values superior to the limits set by the norms for the industrial production of earthenware tiles [12] and the transformation of such mixtures into monolithic ceramics, alone or possibly in mixtures with natural clays, could represent a valid alternative to both landfill disposal and production of cements or concretes.

4. Conclusions

In the present work we have observed that:

- (i) materials obtained from paper mill sludge alone are fractured and not suitable for production of monolithic ceramics;
- (ii) materials obtained from coal fly ash alone can be sintered, but the control of the sintering process is difficult since green bodies shrink and melt in a restricted range of temperatures;
- (iii) intermediate compositions have a progressive shrinkage and fired materials are mainly polycrystalline: their water absorption is low and their mechanical properties are fair. More in particular, the composition containing 25 wt% of coal fly ash and 75 wt% of powders from paper mill sludge show the best overall behaviour.

As a drawback, the shrinkage on firing is high for all the compositions prepared and require optimization.

Acknowledgement

The Italian region Friuli Venezia Giulia is gratefully acknowledged for the financial support.

References

- [1] M. Collepari, Il nuovo calcestruzzo (terza edizione), Ed. Tintoretto, Villorba (TV), 2004.

- [2] L. Barbieri, I. Lancellotti, T. Manfredini, I. Queralt, J.Ma. Rincon, M. Romero, Design, obtainment and properties of glasses and glass-ceramics from coal fly ash, *Fuel* 78 (1999) 271–276.
- [3] J. Sheng, B.X. Huang, J. Zhang, H. Zhang, J. Sheng, S. Yu, M. Zhang, Production of glass from coal fly ash, *Fuel* 82 (2003) 181–185.
- [4] J. Sheng, Vitrification of borate waste from nuclear power plant using coal fly ash. (I) Glass formulation development, *Fuel* 80 (2001) 1365–1369.
- [5] S. Kumar, K.K. Singh, P. Ramachandrarao, Effects of fly ash additions on the mechanical and other properties of porcelainised stoneware tiles, *J. Mater. Sci.* 36 (2001) 5917–5922.
- [6] S.K. Mukherji, B.B. Machhoya, The utilisation of fly ash in the preparation of ceramic tableware and artware, *Br. Ceram. Trans.* 92 (1) (1993) 6–12.
- [7] A. Olgun, Y. Erdogan, Y. Ayhan, B. Zeybek, Development of ceramic tiles from coal fly ash and tincal ore waste, *Ceram Int.* 31 (2005) 153–158.
- [8] C. Marcis, D. Minichelli, S. Bruckner, A. Bachiorrini, S. Maschio, Production of monolithic ceramics from incinerated municipal sewage sludge, paper mill sludge and steelworks slag, *Ind. Ceram.* 25 (2) (2005) 89–95.
- [9] L. Ernstbrunner, Rejects from paper manufacture utilized in the cement works, *Papier* 51 (6) (1997) 284–286.
- [10] C.T. Liaw, H.L. Chang, W.C. Hsu, C.R. Huang, A novel method to reuse paper sludge and cogeneration ashews from paper mill, *J. Hazard. Mater.* 58 (1–3) (1998) 93–103.
- [11] P. Barnes, C. Fentiman, J.W. Jeffery, Structurally related dicalcium silicate phases, *Acta Crystallogr. A* 36 (1980) 353–356.
- [12] T. Manfredini, G.C. Pellacani, Engineering materials handbook, *Ceram. Glasses-ASTM* 4 (1992) 925–929.
- [13] T.W. Cheng, Y.S. Chen, On formation of $\text{CaO-Al}_2\text{O}_3\text{-SiO}_2$ glass-ceramics by vitrification of incinerator fly ash, *Chemosphere* 51 (2003) 817–824.
- [14] T.W. Cheng, Effect of additional materials on the properties of glass ceramic produced from incinerator fly ashes, *Chemosphere* 56 (2) (2004) 127–131.
- [15] T.W. Cheng, T.H. Ueng, Y.S. Chen, J.P. Chiu, Production of glass-ceramic from incinerator fly-ash, *Ceram. Int.* 28 (2002) 779–783.